BIOCHEMISTRY
including biophysical chemistry & molecular biology

Article

pubs.acs.org/biochemistry

Hydrophobicity and Conformational Change as Mechanistic Determinants for Nonspecific Modulators of Amyloid β Self-Assembly

Axel Abelein,[†] Benedetta Bolognesi,[‡] Christopher M. Dobson,[‡] Astrid Gräslund,[†] and Christofer Lendel*[,‡,§]

[†]Department of Biochemistry and Biophysics, Stockholm University, Svante Arrhenius v. 16, SE-106 91 Stockholm, Sweden

[‡]Department of Chemistry, University of Cambridge, Lensfield Road, Cambridge CB2 1EW, U.K.

[§]Department of Molecular Biology, Swedish University of Agricultural Sciences, Uppsala Biomedical Center, Box 590, SE-751 24 Uppsala, Sweden

Supporting Information

ABSTRACT: The link between many neurodegenerative disorders, including Alzheimer's and Parkinson's diseases, and the aberrant folding and aggregation of proteins has prompted a comprehensive search for small organic molecules that have the potential to inhibit such processes. Although many compounds have been reported to affect the formation of amyloid fibrils and/or other types of protein aggregates, the mechanisms by which they act are not well understood. A large number of compounds appear to act in a nonspecific way affecting several different amyloidogenic proteins. We describe here a detailed study of the mechanism of action of one representative compound, lacmoid, in the context of the inhibition of the aggregation of the amyloid β-peptide (Aβ) associated with Alzheimer's disease. We show that lacmoid binds Aβ(1−40) in a surfactant-like manner and counteracts the formation of all types of Aβ(1−40) and Aβ(1−42) aggregates. On the basis of these and previous findings, we are able to rationalize the molecular mechanisms of action of nonspecific modulators of protein self-assembly in terms of hydrophobic attraction and the conformational preferences of the polypeptide.

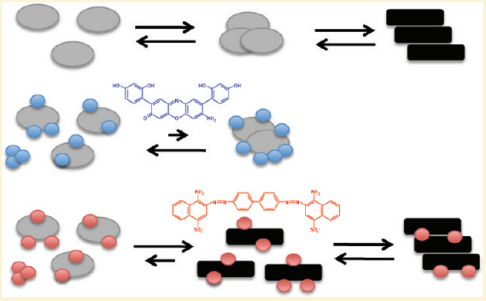

Protein self-assembly leading to highly ordered structures such as amyloid fibrils has developed into a major field of research, primarily because of the link between the formation of such species and a variety of devastating pathological conditions including Alzheimer's and Parkinson's diseases.[1] Despite extensive efforts, the molecular mechanisms of the aggregation processes leading to amyloid structure are not yet fully understood, and the manner in which normally soluble proteins convert into pathogenic species is the subject of intense debate. In some disorders, the extreme load of amyloid material is very likely to be linked directly to the medical symptoms, while other diseases, including the neurodegenerative conditions such as Alzheimer's disease, seem instead to be associated with toxic oligomeric intermediates.[1,2] An understanding of the fundamental mechanisms of amyloid formation and how these processes can be modulated is crucial for major advances in the development of effective therapeutics for this whole class of diseases.

Identification of small organic molecules that disrupt the self-assembly of disease-associated proteins is an attractive approach for developing therapeutics targeting misfolding diseases.[3] Indeed, numerous examples of small molecule inhibitors of protein aggregation have been reported in the literature.[4,5] For the majority of these compounds, however, the inhibitory mechanisms are not yet understood, and detailed biophysical studies of some of the compounds have revealed intriguing mechanisms of action. For example, in a recent investigation of two such molecules, Congo red and lacmoid (Figure 1), in the context of the aggregation of α-synuclein, a protein whose aggregation is associated with Parkinson's disease, we found that both compounds were able by themselves to form supramolecular structures and that this ability was linked to their inhibitory effects on protein aggregation;[6] interestingly, the binding of α-synuclein to these compounds displays clear similarities with its interaction with SDS[7,8] and with lipid vesicles.[9] We were also able to show that, despite the similarities in binding mechanism, the two compounds affect the self-assembly of α-synuclein very differently; Congo red was found

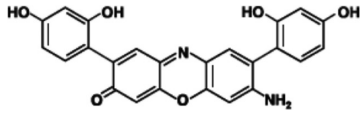

Figure 1. Chemical structure of lacmoid.

Received: November 25, 2011
Revised: December 1, 2011
Published: December 1, 2011

to promote the formation of amorphous aggregates while lacmoid at high concentration inhibits completely the aggregation of the protein.[6] In a subsequent study of the interaction between Congo red and the amyloid β-peptide (Aβ) associated with Alzheimer's disease, we reported[10] a binding mechanism with striking similarities to the interaction between Aβ and low concentrations of sodium dodecyl sulfate (SDS).[11] Specifically, we found that binding to Congo red induces β-sheet conformation in the monomeric peptide and promotes its self-association. The results differed from previously reported inhibitory effects of Congo red on protein aggregation, but other studies have now reported similar findings.[12] These discrepancies illustrate the mechanistic complexity of these types of compounds and indicate further similarities with surfactants that often display such dual behavior.[7,13]

In parallel with our studies, Rao and co-workers demonstrated similar binding characteristics for some other ligands of α-synuclein,[14] and more recently the interaction between Aβ(1−42) and a γ-secretase modulator was shown to rely on small molecule aggregates.[15] In addition, work by Feng et al. revealed a correlation between the ability of small molecules to self-assemble and their inhibiting effect on the formation of fibrils by both yeast and mouse prion proteins.[16] They suggested a mechanism where the proteins are sequestered by large colloidal particles formed by the small molecules, although more recent findings that the diffusion properties of the proteins/peptides do not change dramatically upon complex formation appears to be inconsistent with such a mode of action (refs 6, 10, 17, and 18 as well as current work).

In this paper we describe studies of the interaction between lacmoid and Aβ. Our results show that the binding of lacmoid to monomeric Aβ(1−40), as observed by nuclear magnetic resonance (NMR) spectroscopy, is very similar to that observed for Congo red.[10] The effect on the self-association of Aβ is, however, fundamentally different as we show by several biophysical techniques that lacmoid is able to reduce the formation of amyloid fibrils as well as other types of Aβ aggregates. In the light of these findings and the earlier results described above, we present a molecular hypothesis for the mechanisms of action of nonspecific modulators of protein aggregation in terms of hydrophobic interactions and altered conformational preferences of the polypeptide.

MATERIALS AND METHODS

Materials and Sample Preparation. ^{15}N-labeled and unlabeled Aβ(1−40) peptides for the NMR, circular dichroism (CD), and dynamic light scattering (DLS) experiments were purchased from rPeptide (Bogart, GA) and Alexo-Tech (Umeå, Sweden). Peptides were purified by HPLC by the supplier and used without any further purification. Aβ(1−40) and Aβ(1−42) for the thioflavin T (ThT), CD, and transmission electron microscopy (TEM) studies were purchased from Bachem AG (Bubendorf, Switzerland).

Peptides were stored in solid form at −18 °C and warmed up at room temperature before weighing. The peptides were dissolved in 10 mM NaOH to a final peptide concentration of 1 mg/mL. After 1 min of sonication in a water−ice bath, sodium phosphate buffer and water were added to obtain a final sodium phosphate buffer concentration of 10 mM. This step was followed by a second sonication for 1 min. The pH was adjusted to 7.2 or 7.4 by adding small amounts of NaH_2PO_4 and Na_2HPO_4. Throughout the whole sample preparation the peptides and solvents were kept on ice. The peptide concentrations of the samples were determined by weight.[11]

For NMR measurement, ^2H_2O was added after the first sonication step to obtain a final volume proportion of 10% ^2H_2O. Trimethylsilyl propionate (TSP) was added to a final concentration of 20 μM in the same step to generate a reference signal in the 1D spectrum.

Aβ(1−42) samples for CD spectroscopy and Aβ(1−40) and Aβ(1−42) samples for the ThT and TEM studies were prepared by dissolving 1 g of peptide in 1 mL of trifluoroacetic acid (TFA) and sonicating for 30 s on ice. After removal of the TFA by lyophilization the peptide was dissolved in 1,1,1,3,3,3-hexafluoro-2-propanol (HFIP) and divided into aliquots. The HFIP was then removed by rotary evaporation at room temperature, and the aliquots were stored at −80 °C. Peptide samples were dissolved in 50 mM sodium phosphate buffer, pH 7.4, to obtain a peptide concentration of 30 μM.

Lacmoid was purchased from Sigma (Stockholm, Sweden). 5 mM stock solutions were prepared in 10 mM sodium−phosphate buffer at the same pH as the peptide solutions. For NMR experiments 10% ^2H_2O was added. The solution was sonicated for several hours to dissolve lacmoid particles and stored at room temperature.

SDS was purchased from ICN Biomedicals (Aurora, OH), and 0.1 M stock solutions were prepared in 10 mM sodium phosphate buffer, pH 7.4.

Circular Dichroism. The far-UV CD spectra were acquired with a Chirascan CD spectrometer (Applied Photophysics, Leatherhead, U.K.) equipped with a Peltier temperature control system. Measurements were performed using a cell with a 1 mm optical path length. The spectral region was recorded from 260 to 190 nm with a step size of 0.5 or 1 nm and a bandwidth of 1 or 2 nm. Data were collected with a time of 0.25 s per point, the spectra were averaged over 10 scans, and the background signal was subtracted. The samples used for the time dependence experiments at low temperature were stored on ice or at 8 °C during the investigation. For the time dependence measurements at 37 °C, the samples were kept in the CD cuvettes at this temperature throughout the incubation time.

10 μM Aβ(1−42) samples were allowed to aggregate at 29 °C in 50 mM sodium phosphate buffer, pH 7.4, in the presence or absence of 200 μM lacmoid in an Eppendorf tube. Aliquots were continuously removed and diluted to 5 μM final peptide concentration in a CD cuvette with 1 mm path length. The measurements were performed at 29 °C on an AP Chirascan instrument (Applied Photophysics, Leatherhead, U.K.).

Nuclear Magnetic Resonance. All experiments were performed using pulse sequences in Bruker Topspin 2.1 on Bruker Avance 500, 600, and 700 MHz spectrometers. The 500 and 700 MHz spectrometers were equipped with cryogenic probes. For all 2D NMR experiments spectral widths of at least 11 and 23 ppm were used in the ^{1}H and ^{15}N dimensions, respectively.

^{1}H−^{15}N heteronuclear single quantum coherence (HSQC)[19] spectra at 3 °C were recorded on the 700 MHz spectrometer using 1024 × 64 complex points and 8 scans per transient. Lacmoid was titrated into a sample containing 50 μM ^{15}N-Aβ(1−40) in 10 mM sodium phosphate buffer, pH 7.4, with 10% ^2H_2O to give a final molar ratio of lacmoid to Aβ of 10:1.

^{1}H−^{15}N HSQC[19] and ^{1}H−^{15}N transverse relaxation-optimized spectroscopy (TROSY)[20] experiments at 25 °C were performed using 1024 × 256 complex points with 12 and 16 scans per transient, respectively. Lacmoid was titrated into a sample

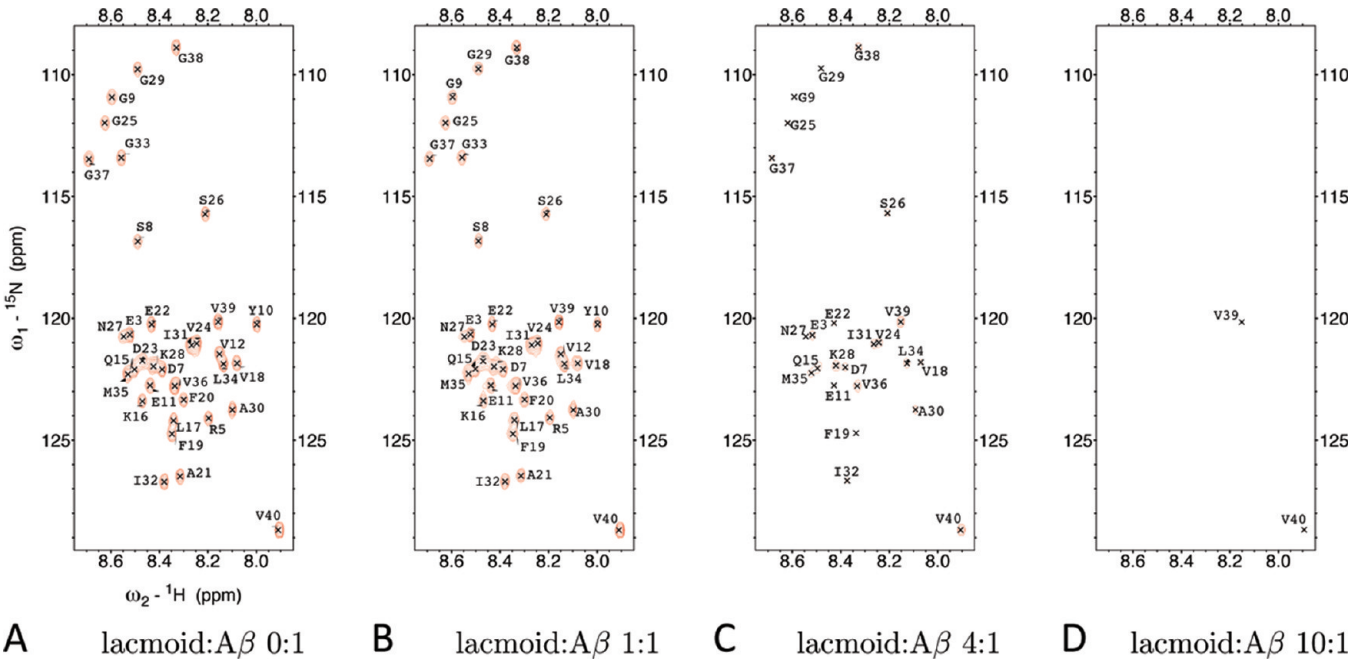

Figure 2. Comparison of $^{1}H-^{15}N$ HSQC NMR spectra of 40 μM Aβ(1−40) without (A) and with 1:1 (B), 4:1 (C), and 10:1 mol equiv (D) of lacmoid. The data were acquired in 10 mM sodium phosphate buffer, pH 7.4, at 3 °C.

containing 50 μM ^{15}N-Aβ(1−40) in 10 mM sodium phosphate buffer, pH 7.2, with 10% $^{2}H_2O$ and 20 μM TSP to give a final ratio of lacmoid to Aβ of 10:1.

The data were processed using NMRPIPE[21] and analyzed in CCPNMR[22] and Sparky 3.114 (T. D. Goddard and D. G. Kneller, SPARKY 3, University of California, San Francisco). The temperature was calibrated to 298 K using a 99.8% deuterated methanol sample.[23]

The weighted average of chemical shift differences was calculated as follows:

$$\Delta\delta_{HN,av} = \sqrt{\frac{1}{2}((\Delta\delta_N/5)^2 + \Delta\delta_H{}^2)}$$

The chemical shift changes and relative intensities were evaluated only for cross-peaks with a sufficient signal-to-noise ratio. At high temperature the intensity and chemical shifts for Q15/M35 and V24/I31 were not evaluated due to cross-peak overlap.

Pulsed field gradient (PFG)[24,25] and saturation transfer difference (STD)[26,27] NMR experiments were measured at 3 °C on unlabeled Aβ(1−40) samples in 10 mM sodium phosphate buffer, pH 7.4 (uncorrected reading), in 100% $^{2}H_2O$ (with the same buffer conditions as above). Lacmoid was titrated into the sample to a final molar ratio of 10:1. The PFG experiments were recorded as a series of 1D ^{1}H spectra of 8K complex points with 10 ppm spectral width, and 128 scans per transient were acquired with the gradient strength varied from 2 to 50 G/cm. The diffusion delay was 100 ms, and the gradient length was 2 ms. The methyl regions of the 1D spectra were integrated and plotted as a function of the gradient strength. Diffusion coefficients were determined by data fitting using Topspin (Bruker). STD NMR spectra were measured with 8K complex points and 10 ppm spectral width; 256 scans per transient were acquired. The off-resonance saturation frequency was set to 43 ppm while on-resonance saturation was applied at 0.533 ppm (methyl) or 6.817 ppm (aromatic). On- and off-resonance experiments were recorded in an interleaved fashion.

Water−amide hydrogen exchange rates for Aβ(1−40) were measured using clean chemical exchange (CLEANEX-PM) experiments with a fast-HSQC detection scheme.[28,29] The experiments were carried out at 5 °C on the 600 MHz spectrometer using 2048 × 104 complex points with 128 scans per transient. After selective water excitation, spectra were acquired with mixing periods, τ_m, of 8, 15, 30, 60, 100, 150, and 300 ms. The water−NH exchange rates k were calculated using nonlinear least-squares fits of the equation

$$\frac{I}{I_0} = \frac{k}{R_{A,app} + k - R_{B,app}}[\exp(-R_{B,app}\tau_m) - \exp(-R_{A,app} + k)\tau_m]$$

where I_0 and I are the peak intensities obtained by fast-HSQC and CLEANEX-PM experiments, respectively. k is the normalized exchange rate constant, and $R_{A,app}$ and $R_{B,app}$ are apparent longitudinal relaxation rates for protein and water, respectively. The apparent relaxation rate for water, $R_{B,app}$, is set to 0.6 s^{-1}.[29] Monte Carlo simulations were performed to determine the average exchange rate k and its variance. Randomly generated noise amplitudes were produced within the maximum signal-to-noise error range for each cross-peak. A normal distribution for the randomly generated noise amplitudes was assumed. The exchange rate k was averaged over 10 000 simulated fitting parameters with the standard deviation given as an error for the exchange rate.

Dynamic Light Scattering. DLS measurements were conducted on an ALV/CGS-3 compact gonimeter system (ALV-GmbH, Langen, Germany) with a HeNe laser operating at 632.8 nm. A scattering angle of 150° was applied, and measurements were performed at 5 and 37 °C for the low- and high-temperature experiments, respectively. The data were analyzed using ALV-500 correlator software.

dx.doi.org/10.1021/bi201745g | *Biochemistry* 2012, 51, 126−137

In the low-temperature experiments, the individual stock solutions (Aβ(1−40), lacmoid, and buffer) were passed through 0.2 μm filters before the final sample preparation. The samples contained 40 μM Aβ(1−40) in 10 mM sodium phosphate buffer, pH 7.4, without or with 200 μM lacmoid and were stored in the same DLS tube on ice or at 8 °C throughout the experiment. The measurements were performed at 5 °C.

DLS measurements of the samples from the 37 °C CD experimental series were measured without any filtration of the samples.

Filtration Experiments. Filtration experiments were performed using inorganic membrane filters with cutoff sizes of 20 and 200 nm (Whatman GmbH, Dassel, Germany). The absorbance of Aβ(1−40) and lacmoid was measured on a Jasco V-560 UV/vis spectrometer at room temperature. The presence of lacmoid was determined from the absorbance at 593 ± 1 nm while the presence of peptide was monitored with CD and shown as the percentage of the CD signal at 197 ± 1 nm of pure, unfiltered Aβ. The samples contained 50 μM Aβ(1−40) in 10 mM sodium phosphate buffer, pH 7.4, with or without 100 μM lacmoid. CD measurements were conducted at low temperature (5 or 10 °C). Peptide absorbance was also measured at the tyrosine maximum at 274.5 nm.

ThT Fluorescence Assays. Aβ peptide was dissolved in 20 μM ThT in 50 mM sodium phosphate buffer, pH 7.4, and directly aliquoted into 96-well Costar plates. The plates were incubated at 29 °C in a FLUOstar OPTIMA plate reader (BMG LabTech, Offenburg, Germany) where fluorescence measurements were performed with different time intervals with excitation at 440 nm, emission at 480 nm, 10 flashes/well, and three different gains (1500, 2000, and 2500). Plates were shaken for 10 s every 5 min during incubation.

Transmission Electron Microscopy. Samples of 10 μL of aggregated peptide solution were deposited on Formvar/Cu^{2+} grids and left for 2 min. The grids were washed twice with distilled filtered water. In order to stain the amyloid fibrils negatively, 10 μL aliquots of uranyl acetate 2% (w/v) were deposited on the grid and left for 2 min before drying in air. Grids were stored at room temperature until examination in a Philips CM100 TEM microscope, operating at 80 keV.

Calculation of log *P* Values. Theoretical octanol:water partitioning coefficients (log *P*) for the molecules were calculated using MarvinSketch 5.5.0.1 (ChemAxon Ltd.). For simplicity, only the major protonation microspecies, as identified by the software at pH 7.4, was considered. The log *P* values were calculated using the weighted method (equal weights of the VG, KLOP, and PHYS methods) with electrolyte concentrations of 0.1 M for both anions and cations. Molecules involving coordinated metal ions were excluded from the analysis of compounds listed by Masuda et al.[4] and Necula et al.[5]

RESULTS

Lacmoid Forms Supramolecular Structures in Solution. In previous work we showed that lacmoid in aqueous solution forms supramolecular structures.[6] Using DLS, we confirmed that this ability is retained also under the experimental conditions of the present study, as exemplified by the results presented in Supporting Information Figure S1. Evaluation of the scattering data of lacmoid in the presence and absence of Aβ(1−40) gives polydispersed size distributions suggesting that a number of different species exist in the samples, including large particles (hydrodynamic radius $R_H \approx 50-100$ nm) as well as smaller entities with R_H in the range of 1−10 nm (Supporting Information Figure S1). In addition, previous NMR experiments suggest that monomeric and/or small oligomeric lacmoid assemblies are also present in solution.[6]

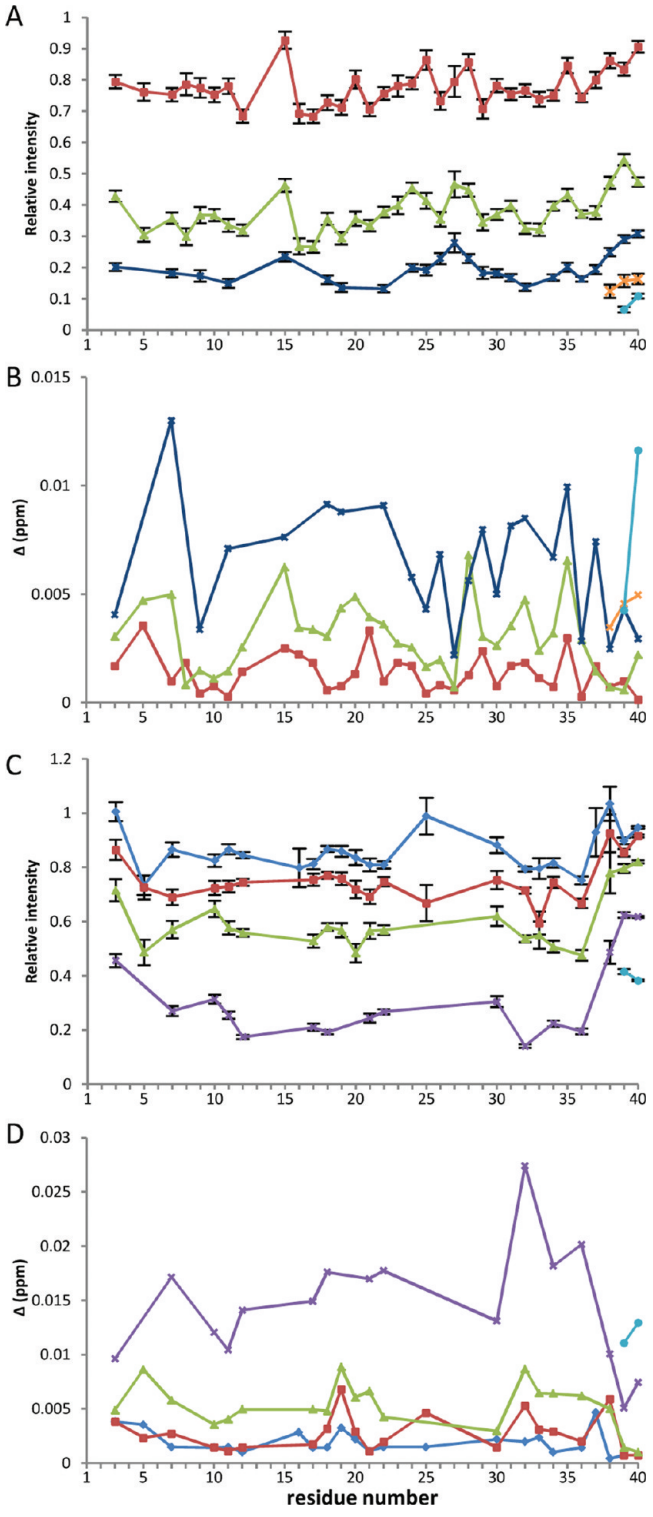

Figure 3. Changes in $^1H-^{15}N$ HSQC cross-peak intensities (A, C) and chemical shifts (B, D) of Aβ(1−40) as a function of added lacmoid. (A, B) Spectra of 40 μM Aβ(1−40) acquired at 3 °C. (C, D) Spectra of 50 μM Aβ(1−40) acquired at 25 °C. The colors represent 0.5:1 (light blue), 1:1 (red), 2:1 (green), 4:1 (dark blue), 5:1 (violet), 6:1 (orange), and 10:1 mol equiv (turquoise) of lacmoid added. The error bars indicate the signal-to-noise ratios.

Binding of Lacmoid to Monomeric Aβ Investigated by NMR. NMR spectroscopy was used to monitor lacmoid binding

dx.doi.org/10.1021/bi201745g | *Biochemistry* 2012, 51, 126−137

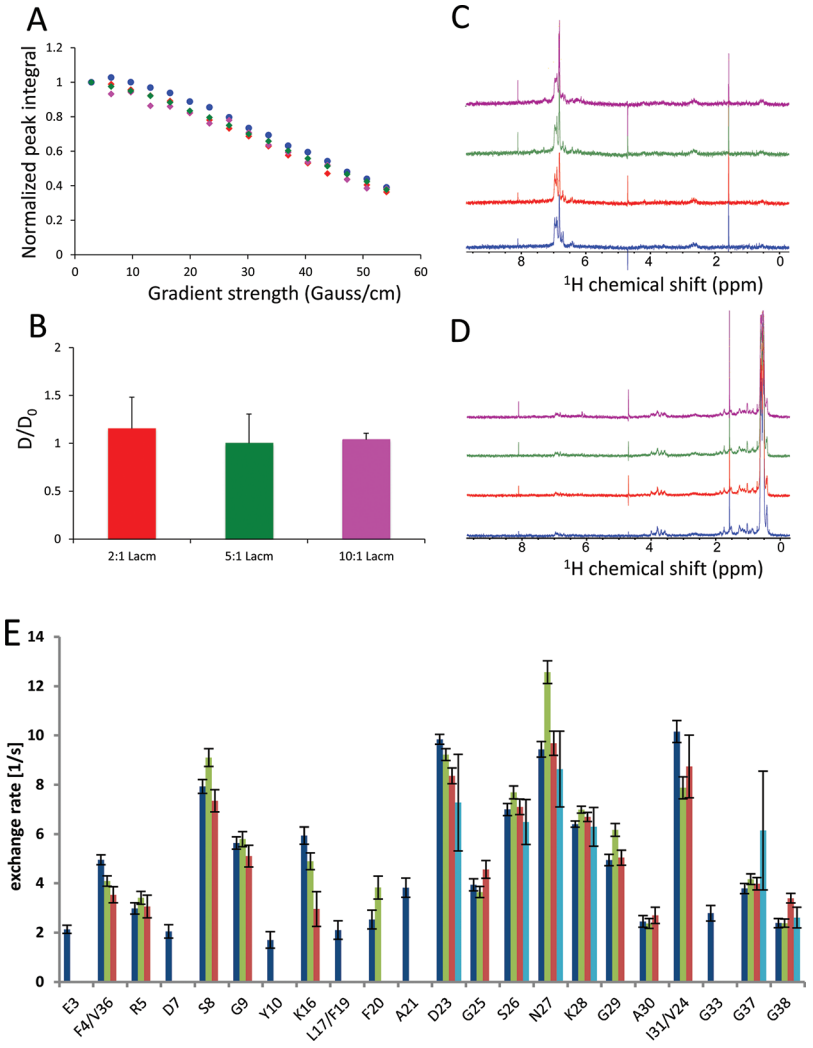

Figure 4. (A, B) PFG NMR experiments carried out at 3 °C on a sample containing 50 μM Aβ(1−40) in 10 mM sodium phosphate buffer, pH 7.4, with gradual addition of up to a 10:1 mol equiv of lacmoid. (A) The integrals of the methyl region of the ^{1}H spectrum plotted against the applied gradient strength for Aβ reference sample (blue) and with 2:1 (red), 5:1 (green), and 10:1 (magenta) mol equiv of lacmoid. (B) Relative diffusion coefficient values of Aβ(1−40) in the presence of increasing molar ratios of lacmoid compared to control samples without lacmoid. (C, D) Only minor peaks appear in the STD NMR spectrum when the aromatic (C) or methyl (D) regions of the ^{1}H spectrum of Aβ(1−40) are saturated. Spectra shown for 50 μM Aβ(1−40) sample without lacmoid (blue) and with 2:1 (red), 5:1 (green), and 10:1 mol equiv (magenta) of lacmoid. (E) Amide proton exchange rates measured by CLEANEX-PM for 50 μM Aβ(1−40) in 10 mM sodium phosphate buffer, pH 7.2, without (blue) and with 50 (green), 100 (red), and 500 μM (turquoise) lacmoid.

to Aβ(1−40) at atomic resolution. The experiments were mainly carried out at low temperature (3 °C) to minimize NMR signal loss due to amide hydrogen exchange with water and effects originating from peptide self-association.

The ^{1}H−^{15}N HSQC spectrum of monomeric Aβ(1−40) is well dispersed (Figure 2A) and provides an opportunity of mapping ligand binding sites onto the Aβ sequence. The addition of increasing amounts of lacmoid to the Aβ(1−40) sample results in concentration-dependent decreases of cross-peak intensities throughout the whole spectrum (Figures 2 and 3A) in a similar way to those previously reported for Congo red[10] and for low concentrations of SDS.[11] While the peak intensities are strongly affected by binding, the chemical shifts of the cross-peaks display only minor perturbations (Figure 3B), although these perturbations increase with increasing concentrations of lacmoid. The ^{1}H−^{15}N HSQC experiments were repeated at 25 °C, and we observe similar intensity changes to those observed at low temperature (Figure 3C,D and Figure S2). In an attempt to enhance the peak intensities in the ^{1}H−^{15}N correlation NMR spectra, we carried out TROSY experiments that have the ability to improve cross-peak intensities of large molecular species.[20] The TROSY results follow the same trend as those in the HSQC spectra (Figures S3 and S4A,B), suggesting that the line broadening cannot only be attributed to the formation of high molecular weight complexes.

Further evidence for the small size of the Aβ(1−40):lacmoid complex comes from PFG NMR[24,25] and STD experiments.[26,27] The PFG measurements show no indications of any significant difference in the diffusion properties of Aβ(1−40) as seen in the remaining NMR signal whether or not lacmoid is bound (Figure 4A,B), and the STD spectra display no signal enhancements as a function of the increased lacmoid concentration (Figure 4C,D) as would be expected for large and compact molecular complexes.

In order to explore whether or not lacmoid binding induces any structural rearrangement or partial folding of Aβ(1−40),

dx.doi.org/10.1021/bi201745g | *Biochemistry* 2012, 51, 126−137

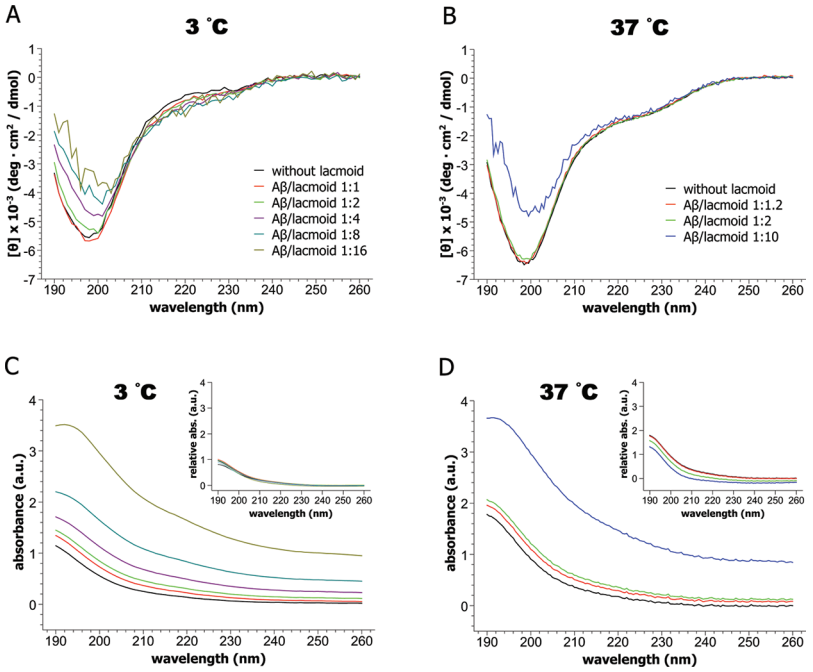

Figure 5. Far-UV CD spectra (A, B) and the corresponding absorbance spectra (C, D) of Aβ(1−40) in 10 mM sodium phosphate buffer in the presence of different concentrations of lacmoid. The graphs inserted in (C, D) show the relative absorbance when the lacmoid background absorbance is subtracted. (A, C) 40 μM Aβ at 3 °C. (B, D) 50 μM Aβ at 37 °C.

we measured the exchange rates between Aβ(1−40) amide hydrogen atoms and water in the presence and absence of lacmoid using CLEANEX-PM experiments with a fast-HSQC detection scheme.[28,29] We find that the exchange rates of free Aβ(1−40) vary by factors of up to 5 along the peptide sequence (Figure 4E) but that the rates are not changed by the addition of increasing amounts of lacmoid (Figure 4E and Figure S4C). Hence, we conclude that binding of lacmoid does not induce any structural changes in Aβ(1−40) in any manner that alters the protection of the amide protons from water exchange.

Taken together, the NMR investigations of the interaction between Aβ(1−40) and lacmoid shows that binding is primarily manifested by reduced peak intensities that are seen for residues throughout the sequence. The reduced peak intensity cannot be attributed either to changes in amide proton hydrogen exchange rates or to an increase in molecular dimension but rather to effects of intermediate to slow conformational exchange, either between free and bound Aβ(1−40) molecules or between several different conformations in the structural ensemble of the peptide. The most C-terminal residues are less affected, indicating that they are not directly involved in binding or that they retain more of their native flexibility. The finding that Aβ:lacmoid complexes are small (i.e., of similar dimension to the free peptide) is further supported by filtration experiments showing that despite the fact that a significant amount of lacmoid molecules in a 100 μM sample is retained by a filter with 20 nm cutoff, the presence of the same concentration of lacmoid does not alter the ability of Aβ(1−40) to pass through the filter (Figure S5). Hence, we conclude that binding of lacmoid to Aβ proceeds via monomeric or small oligomeric species, which is in agreement with our previous observations for the binding of Congo red to Aβ(1−40),[10] the interactions of lacmoid and Congo red with α-synuclein,[6] and recent findings from other groups.[17,18]

Effect of Lacmoid Binding on the Secondary Structure of Aβ(1−40). The NMR data described above provide no evidence for any alteration of secondary structure upon lacmoid binding to Aβ(1−40), but such evidence would almost certainly be hidden by the effects of the extensive line broadening. We therefore made use of far-UV CD spectroscopy to investigate how lacmoid affects the conformational properties of Aβ(1−40) at a global level.

The experiments were carried out at low (3 °C) and high (37 °C) temperatures. The CD spectrum of free Aβ(1−40) is characterized by the existence of predominately random coil-like structure with some contribution of PII-helix that becomes more populated at lower temperatures.[30] Addition of increasing concentrations of lacmoid causes changes in the 190−200 nm region of the CD spectrum while leaving the region around 215−225 nm, which is indicative of ordered α-helical and β-sheet structure, essentially unaffected (Figure 5A,B), indicating that no persistent secondary structure is induced upon binding. Notably, at the higher temperature no changes occur at all until the lacmoid concentration reaches 500 μM. The decreased amplitude of the spectrum at shorter wavelengths (190−210 nm) indicates that some more subtle structural changes might occur. However, the signal-to-noise ratio of this particular region of the spectrum decreases as the lacmoid concentration increases, an effect that can be attributed to light scattering effects by lacmoid particles (Figure 5C,D). Comparison with samples of lacmoid in buffer shows that the scattering effect is due to aggregates of lacmoid and does not involve formation of peptide aggregates (Figure 5C,D insets). As light scattering can cause changes in the observed CD spectrum of polypeptides,[31] however, it is difficult to speculate on the exact nature and extent of the conformational transitions underlying the alteration in the 190−210 nm spectral region.

Inhibition of Aβ Aggregation by Lacmoid Observed by Thioflavin T Fluorescence and Electron Microscopy. To explore the effect of lacmoid on Aβ amyloid formation, the fluorescence of the amyloid reporting dye ThT was monitored as a function of time in samples of Aβ(1−40) and Aβ(1−42) incubated with and without lacmoid at 29 °C (Figure 6A). Although significantly reduced ThT fluorescence was observed

dx.doi.org/10.1021/bi201745g | *Biochemistry* 2012, 51, 126−137

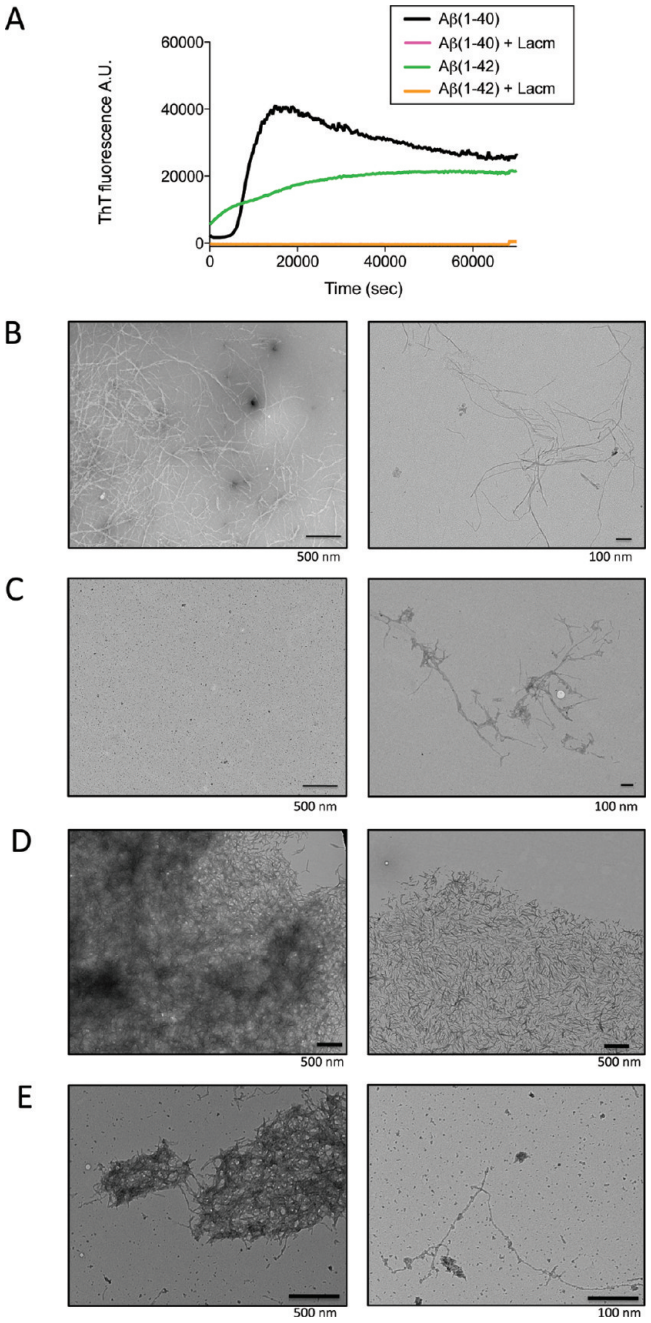

Figure 6. (A) Kinetic traces of Aβ fibril formation at 29 °C monitored by ThT fluorescence. Black and green lines represent control samples with 30 μM Aβ(1−40) and Aβ(1−42), respectively. Samples with a 10-fold molar excess of lacmoid added are displayed in magenta for Aβ(1−40) and orange for Aβ(1−42). (B, C) TEM images of 10 μM Aβ(1−40) incubated without (B) or with (C) 100 μM lacmoid. Left and right images represent different magnifications. (D, E) TEM images of 30 μM Aβ(1−42) without (D) or with (E) 300 μM lacmoid. Left and right images in (E) represent different magnifications.

in the presence of lacmoid, this observation does not represent strong evidence for the inhibitory effect of the compound, as interference between dye molecules, such as lacmoid or Congo red, and ThT, by binding site competition, fluorescence quenching, or direct interactions between dye molecules, has previously been demonstrated by us and others.[6,10,32]

Aβ samples incubated with and without lacmoid were therefore also investigated using TEM. While images of samples containing only Aβ(1−40) or Aβ(1−42) reveal the presence of amyloid fibrils, samples incubated in the presence of lacmoid clearly display substantially reduced amounts of aggregated material (Figure 6B−E). Notably, we do not observe any large (R_H = 50−100 nm) lacmoid particles by TEM, but the dotlike structures in Figure 6C,E could indeed be smaller lacmoid assemblies. Taken together, the experiments suggest an inhibitory effect for lacmoid on Aβ self-assembly. To confirm this finding and to acquire a more detailed knowledge of the inhibition mechanism, the ThT and TEM experiments were supplemented by studies using far-UV CD and DLS.

Kinetics of Aβ Amyloid Formation Investigated by CD and DLS. Samples of Aβ(1−40) incubated at 37 °C without and with 60 and 500 μM lacmoid were studied using far-UV CD spectroscopy over a period of 26 days. During this period we observed extensive structural conversions in the samples without and with 60 μM lacmoid, resulting in a broad spectral minimum between 206 and 215 nm (Figure 7A,B), signifying a β-sheet-rich structure as reported for aged Aβ(1−40) samples under similar conditions.[33] As described above, the signal-to-noise level of the sample with 500 μM lacmoid is low. However, the CD spectra report no indication of any significant changes in the 215−225 nm spectral region, suggesting that Aβ(1−40) retains its random coil characteristics (Figure 7C). After the incubation period, the samples from the CD study were also investigated by DLS. Comparisons of the autocorrelation functions show a shift toward shorter correlation times as the concentration of lacmoid increases (Figure 7D), a finding that is in agreement with the reduced formation of peptide aggregates in the presence of lacmoid. Hence, CD and DLS data strongly suggest that lacmoid counteracts the self-assembly and amyloid formation of Aβ(1−40).

Samples of Aβ(1−40) containing increasing amounts of lacmoid were also followed by far-UV CD spectroscopy at low temperature (the measurements were carried out at 3 °C, and the samples were stored at 5−8 °C) to confirm an inhibitory effect of lacmoid under the experimental conditions used for the NMR study described above. As expected, the structural changes in Aβ(1−40) occur much more slowly at low temperature, but as reported previously,[10] Aβ(1−40) in isolation begins to convert into β-sheet structure during this incubation time (Figure S6A). The presence of lacmoid slows down the structural conversion (Figure S6B−F) and thereby confirms the results of the high-temperature experiments. The time dependence of the DLS intensity (count rate) was also followed for separate samples containing Aβ(1−40) with and without lacmoid and incubated at low temperature (Figure S6G). The results show that the sample containing lacmoid initially scatters more light than the control sample. The scattering intensity of this sample is, however, constant over time while the Aβ sample without lacmoid display increased light scattering indicating the formation of peptide aggregates.

Finally, we confirm that the observed inhibitory effect of lacmoid is also valid for the kinetics of the self-assembly of Aβ(1−42). Samples of Aβ(1−42) with and without 10:1 molar excess of lacmoid were incubated at 29 °C. Aliquots were collected at several time points and analyzed by CD spectroscopy. The results are presented in Figure S7 and show that the conversion into β-sheet structure is slower in the sample containing lacmoid and, more importantly, the extent of β-sheet material is reduced, as shown by the fact that the amplitude of the CD spectrum is approximately half of that of the sample with Aβ(1−42) alone.

dx.doi.org/10.1021/bi201745g | *Biochemistry* 2012, 51, 126−137

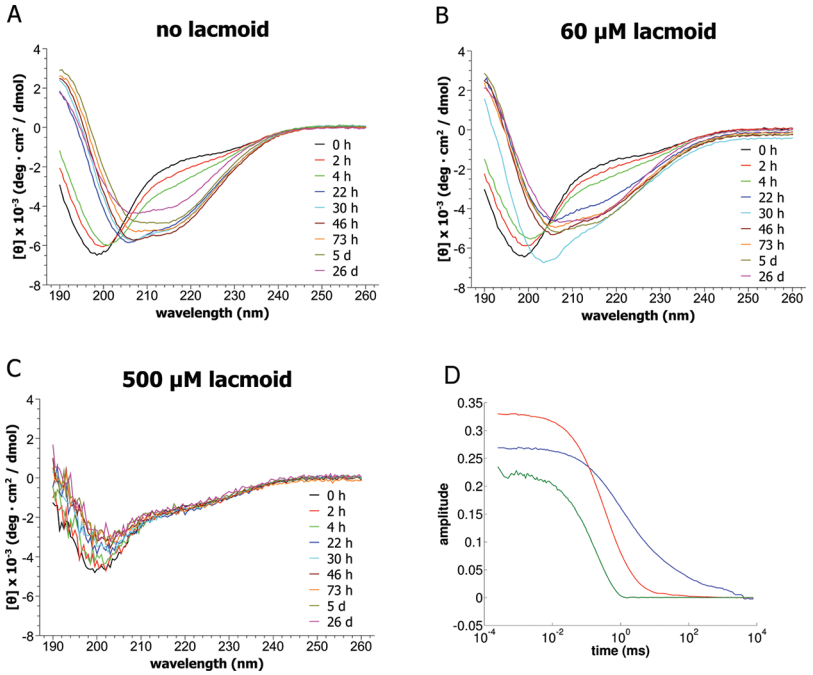

Figure 7. (A–C) Time dependence of the far-UV CD spectrum of 50 μM Aβ(1–40) incubated in 10 mM sodium phosphate buffer, pH 7.2, at 37 °C without (A) and with 60 μM (B) and 500 μM (C) lacmoid. The samples were monitored over a period of 26 days. (D) DLS autocorrelation functions of the CD samples at the end of the incubation period. Aβ without (blue) and with 60 (red) and 500 μM (green) lacmoid.

Competition with SDS Binding. Aβ interacts with SDS micelles, and the interaction is accompanied by a structural transition into α-helical structure.[11,34] To obtain further insights into the interaction mechanisms of lacmoid and Congo red with Aβ, we investigated the competition of the binding of Aβ(1–40) to lacmoid/Congo red and to SDS micelles. Addition of a micelle forming concentration (10 mM) of SDS to monomeric Aβ(1–40) in solution changes the far-UV CD spectrum from one typical of a random-coil to one characteristic of α-helical structure, as previously reported.[11] In freshly prepared samples of Aβ(1–40) with Congo red or lacmoid we observe similar transitions (data not shown), indicating that none of the compound is able to compete with the SDS binding to the monomeric peptide. We further tested the SDS binding competition with aged (77 days) Aβ(1–40) samples incubated at low temperature with Congo red or lacmoid. Peptide samples incubated with Congo red display a strong β-sheet-like spectrum that is only marginally changed by the addition of SDS (Figure 8B). This result indicates that the Aβ aggregates formed in presence of Congo red[10] are very stable and are not disrupted by the detergent. The samples incubated with lacmoid still display a CD spectrum typical of an unstructured peptide, but this spectrum changes to have α-helical-like character when 10 mM SDS is added (Figure 8A), indicating that Aβ is still able to access its native, helical, SDS-associated structure.

DISCUSSION

Conformational Change and Aβ Self-Assembly. Elucidation of the mechanisms by which soluble monomeric Aβ converts into higher order aggregates is a key question in the context of the molecular origins of Alzheimer's disease. Aβ is a highly flexible peptide that can adopt a number of different conformational states, making structural characterization a highly challenging task. The presence of other molecules, that either bind directly to Aβ or alter the properties of the solution, makes the system even more complex.

In solution, monomeric Aβ displays random coil-like characteristics essentially without any persistent secondary or tertiary structure. β-Sheet structure can be induced in the peptide, for example, in the presence of lipid membranes[35] or low concentrations of SDS[11,36,37] or as a consequence of binding to compounds such as Congo red.[10] All these processes also promote Aβ assembly although the aggregates formed may display features that are distinct from those of amyloid fibrils formed by the peptide alone;[12,38] formation of β-sheet structure is therefore, at least in these cases, intimately linked to self-association. By contrast, formation of helical structure is in general protective against polypeptide aggregation; this conclusion has been demonstrated in studies of the effects on Aβ self-assembly of detergents, such as SDS,[11] organic cosolvents, such as trifluorethanol,[39] and other designed molecules.[40]

The results of our extensive series of experiments clearly show that binding of lacmoid does not significantly perturb the random coil characteristics of Aβ, and such conservation of the disordered native state of the peptide could potentially counteract its self-assembly. Recent insights into the aggregation process of Aβ show, however, that retention of the conformational disorder *per se* is not enough to protect the peptide from aggregation as the formation of random coil-like aggregates can eventually lead to amyloid formation.[41] The conversion into β-structure is, however, a key event that in many cases could be the rate-limiting step of the amyloid formation process.[41,42] Hence, stabilization of a random coil structure could have a protective effect with respect to *amyloid* formation but does not account for the inhibition of the assembly of disordered aggregates, for which additional solubilizing effects must also be considered.

Hydrophobicity among Aggregation Inhibitors. It is well-known that many lipids and surfactants interact with amyloidogenic proteins and modulate their self-assembly.[13]

dx.doi.org/10.1021/bi201745g | *Biochemistry* 2012, 51, 126–137

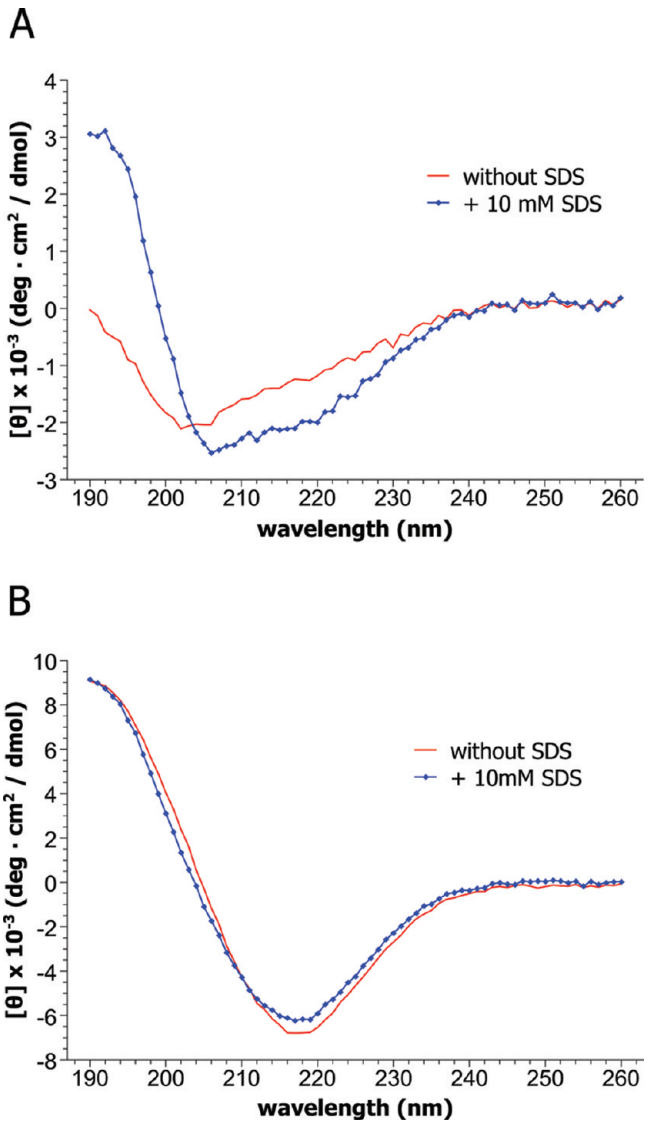

Figure 8. Far-UV CD spectra of 40 μM Aβ(1−40) incubated with 80 μM lacmoid (A) or 80 μM Congo red (B) for 77 days at low temperature before (red line) and after (blue line) the addition of 10 mM SDS. The measurements were carried out at 20 °C.

A recent study has investigated the effects of a range of detergents and amphiphilic molecules on the aggregation of apolipoprotein C-II,[43] and some compounds were found to promote and others to inhibit aggregation of the protein. To rationalize the effects, the authors calculated the hydrophobicity of the molecules as the octanol:water partitioning coefficients (log P) and found that, although both inhibitors and promotors can be hydrophilic as well as hydrophobic, on average the inhibitors are more hydrophobic. Using the same method to calculate log P (MarvinSketch 5.5.0.1, ChemAxon Ltd.) for lacmoid and Congo red, we find that both compounds are hydrophobic (log P = 3.35 and 2.36, respectively). We then extended the calculations to a number of compounds previously reported to affect Aβ aggregation. Necula and co-workers reported three classes of inhibitors of Aβ(1−42) self-assembly based on the ability of the compounds to counteract the formation of oligomers or fibrils or both.[5] Comparing the log P values for these three groups, we find that all compounds that inhibit formation of both oligomers and fibrils have log $P > 0$ (i.e., are hydrophobic) while the other two classes show a larger spread of values of log P (Figure S8A). We also calculated the log P values for the compounds investigated by Masuda et al.[4] in a study in which a large number of molecules were investigated with respect to their effect on the aggregation of three amyloidogenic proteins: α-synuclein, Aβ(1−40), and tau. From our calculations we find that the compounds that affect all three proteins again tend to cluster at positive log P values while compounds without any inhibitory effect, or those affecting only one or two of the proteins, have a greater variety of log P values (Figure S8B). Taken together, it appears that nonspecific inhibitors of polypeptide self-association, including lacmoid and Congo red, in general have a hydrophobic nature although the mechanisms of action for each of the molecules listed in the mentioned references remain to be investigated in detail.

A Molecular Mechanism of Action for Nonspecific Modulators of Protein Aggregation. The hydrophobic effect is a major driving force for the self-assembly of many aggregation prone polypeptides including Aβ.[42,44,45] The generic hydrophobic nature of many of the compounds discussed in the previous section indeed explains the frequent occurrence of self-associating molecules among reported inhibitors of polypeptide aggregation. Furthermore, it suggests that these molecules could bind nonspecifically to hydrophobic surfaces of peptides and proteins, either as monomers or in oligomeric forms, in a similar way to that described for many surfactants.[13] Such binding would undoubtedly modulate the ability of the molecules concerned to interact with each other, either by solubilizing the polypeptide chain and making it less aggregation prone or by promoting its assembly into mixed micelles. Moreover, formation of amyloid-like structures also requires a conformational change into β-sheet structure and the nature of the intrinsic secondary structure propensities is among the determinants of polypeptide amyloidogenicity.[42,45] Nonspecific binding of amphipathic ligands to the protein can affect its conformational properties, either directly, as in the case of Congo red binding to Aβ,[10] or indirectly by strengthening inter- or intramolecular hydrogen bonds[13] and thereby modulating the ability of the polypeptide chain to undergo the structural transitions required to form β-sheet-rich aggregates and eventually amyloid fibrils. Hence, the overall effect of nonspecific, surfactant-like compounds depends on how they modulate the hydrophobic attraction between polypeptide molecules as well as their conformational preferences. This dual effect on the aggregation process can therefore result in different types of behavior of the compounds depending on their concentration, as reported for Congo red[46−48] and many surfactants.[7,11,49]

Protein polymerization processes are governed by a set of microscopic rate constants describing primary and secondary nucleation steps, including breakage, and the subsequent elongation of the resulting aggregates.[50−53] Nonspecific binding of small molecules to the monomeric protein, as described here and in our previous work, is likely to alter directly the nucleation processes as well as the elongation rate. Figure 9 illustrates how the molecular mechanisms described above (i.e., the hydrophobic attraction and the conformational preferences of the polypeptide) could affect the primary nucleation events, which are critical steps in all protein aggregation processes although secondary nucleation processes are often rate limiting for the proliferation of fibrils;[50] an analogous scheme could easily be generated to describe the addition of monomers to small aggregates once these species have formed fibrillar seeds. Interpreting our data for Aβ, Congo red, and lacmoid within the context of such a molecular framework leads to the following

conclusions: As is evident from our CD, DLS, and TEM experiments, lacmoid has the ability to inhibit completely the aggregation process of Aβ, suggesting that it can bind to the exposed hydrophobic surfaces of the peptide molecule, thus favoring its monomeric state (Figure 9B). In addition, binding

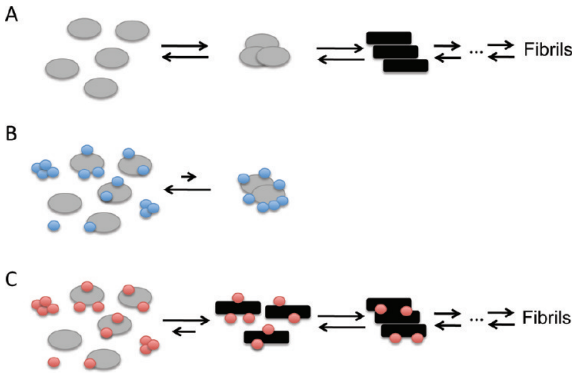

Figure 9. Schematic illustration of a simplified molecular model of Aβ self-assembly. (A) Collisions of monomeric Aβ molecules (gray) lead to the formation of small aggregates of the peptide through a nucleation process. The resulting aggregates undergo a conformational change to form β-sheet-rich aggregates (black) that grow and eventually form amyloid fibrils. (B) Nonspecific binding of monomers or small oligomers of lacmoid (blue) to Aβ reduces the attractive forces between Aβ molecules leading to inhibition of the formation of peptide aggregates. (C) Congo red (red), by contrast, promotes β-sheet structure in monomeric Aβ and increases the rate of the conformational change and thereby the overall process of amyloid formation.

to lacmoid might stabilize a random coil conformation and thereby further counteract the formation of amyloid-like structures. Congo red, on the other hand, induces β-structure even in the monomeric peptide,[10] which accelerates the conformational change necessary to form amyloid structures and thereby reducing the lifetime of less ordered oligomeric states (Figure 9C). Interestingly, Congo red was found not to affect the elongation rate of Aβ(1−42),[32] indicating that, at least for this peptide variant, the effect on nucleation is most critical. In addition, the well-known binding of Congo red to amyloid fibrils[46] could also affect breakage-related or surface-catalyzed secondary nucleation processes.[50] Taken together, the insights gained in the present study provide a molecular framework for interpreting the mechanisms of action of nonspecific modulators of amyloid formation as well as for developing a deeper understanding of the basic principles of protein self-assembly.

■ ASSOCIATED CONTENT

Supporting Information

Figures showing DLS data, additional NMR and CD data, the results of filtration experiments, and statistical analysis of the hydrophobicity of small molecules previously reported to modulate protein aggregation. This material is available free of charge via the Internet at http://pubs.acs.org.

■ AUTHOR INFORMATION

Corresponding Author

*E-mail: lendel@kth.se or christofer.lendel@slu.se. Phone: +46-18-4714489.

Funding

We acknowledge financial support from the Swedish Research Council (A.G. and C.L.), EMBO (C.L.), the Swedish Brain Foundation (A.G.), the Alzheimer's Research Trust (UK) (B.B. and C.M.D.), and the Welcome Trust (C.M.D.).

■ ACKNOWLEDGMENTS

We thank Torbjörn Astlind (Stockholm University) for assistance with the NMR measurements and Tuomas Knowles (University of Cambridge) for comments on the manuscript.

■ ABBREVIATIONS

Aβ, amyloid β; CD, circular dichroism; CLEANEX-PM, clean chemical exchange; DLS, dynamic light scattering; HFIP, 1,1,1,3,3,3-hexafluoro-2-propanol; HSQC, heteronuclear single quantum coherence; log *P*, octanol:water partitioning coefficient; NMR, nuclear magnetic resonance; PFG, pulsed field gradient; SDS, sodium dodecyl sulfate; STD, saturation transfer difference; TEM, transmission electron microscopy; TFA, trifluoroacetic acid; ThT, thioflavin T; TROSY, transverse relaxation-optimized spectroscopy; TSP, trimethylsilyl propionate.

■ REFERENCES

(1) Chiti, F., and Dobson, C. M. (2006) Protein misfolding, functional amyloid, and human disease. *Annu. Rev. Biochem. 75*, 333−366.

(2) Walsh, D. M., and Selkoe, D. J. (2007) Aβ oligomers - a decade of discovery. *J. Neurochem. 101*, 1172−1184.

(3) Dobson, C. M. (2004) Protein chemistry. In the footsteps of alchemists. *Science 304*, 1259−1262.

(4) Masuda, M., Suzuki, N., Taniguchi, S., Oikawa, T., Nonaka, T., Iwatsubo, T., Hisanaga, S., Goedert, M., and Hasegawa, M. (2006) Small molecule inhibitors of α-synuclein filament assembly. *Biochemistry 45*, 6085−6094.

(5) Necula, M., Kayed, R., Milton, S., and Glabe, C. G. (2007) Small molecule inhibitors of aggregation indicate that amyloid β oligomerization and fibrillization pathways are independent and distinct. *J. Biol. Chem. 282*, 10311−10324.

(6) Lendel, C., Bertoncini, C. W., Cremades, N., Waudby, C. A., Vendruscolo, M., Dobson, C. M., Schenk, D., Christodoulou, J., and Toth, G. (2009) On the mechanism of nonspecific inhibitors of protein aggregation: dissecting the interactions of α-synuclein with Congo red and Lacmoid. *Biochemistry 48*, 8322−8334.

(7) Rivers, R. C., Kumita, J. R., Tartaglia, G. G., Dedmon, M. M., Pawar, A., Vendruscolo, M., Dobson, C. M., and Christodoulou, J. (2008) Molecular determinants of the aggregation behavior of α- and β-synuclein. *Protein Sci. 17*, 887−898.

(8) Ulmer, T. S., Bax, A., Cole, N. B., and Nussbaum, R. L. (2005) Structure and dynamics of micelle-bound human α-synuclein. *J. Biol. Chem. 280*, 9595−9603.

(9) Bodner, C. R., Dobson, C. M., and Bax, A. (2009) Multiple tight phospholipid-binding modes of α-synuclein revealed by solution NMR spectroscopy. *J. Mol. Biol. 390*, 775−790.

(10) Lendel, C., Bolognesi, B., Wahlström, A., Dobson, C. M., and Gräslund, A. (2010) Detergent-like interaction of Congo red with the amyloid β peptide. *Biochemistry 49*, 1358−1360.

(11) Wahlström, A., Hugonin, L., Peralvarez-Marin, A., Jarvet, J., and Gräslund, A. (2008) Secondary structure conversions of Alzheimer's Aβ(1−40) peptide induced by membrane-mimicking detergents. *FEBS J. 275*, 5117−5128.

(12) Bose, P. P., Chatterjee, U., Xie, L., Johansson, J., Göthelid, E., and Arvidsson, P. I. (2010) Effects of congo red on Aβ1−40 fibril formation process and morphology. *ACS Chem. Neurosci. 1*, 315−324.

(13) Otzen, D. E. (2010) Amyloid formation in surfactants and alcohols: membrane mimetics or structural switchers? *Curr. Protein Pept. Sci. 11*, 355−371.

(14) Rao, J. N., Dua, V., and Ulmer, T. S. (2008) Characterization of α-synuclein interactions with selected aggregation-inhibiting small molecules. *Biochemistry 47*, 4651−4656.

(15) Barrett, P. J., Sanders, C. R., Kaufman, S. A., Michelsen, K., and Jordan, J. B. (2011) NSAID-based γ-secretase modulators do not bind to the amyloid-β polypeptide. *Biochemistry 50*, 10328−10342.
(16) Feng, B. Y., Toyama, B. H., Wille, H., Colby, D. W., Collins, S. R., May, B. C., Prusiner, S. B., Weissman, J., and Shoichet, B. K. (2008) Small-molecule aggregates inhibit amyloid polymerization. *Nat. Chem. Biol. 4*, 197−199.
(17) Pedersen, M. O., Mikkelsen, K., Behrens, M. A., Pedersen, J. S., Enghild, J. J., Skrydstrup, T., Malmendal, A., and Nielsen, N. C. (2010) NMR reveals two-step association of Congo Red to amyloid beta in low-molecular-weight aggregates. *J. Phys. Chem. B 114*, 16003−16010.
(18) Lamberto, G. R., Torres-Monserrat, V., Bertoncini, C. W., Salvatella, X., Zweckstetter, M., Griesinger, C., and Fernandez, C. O. (2011) Toward the discovery of effective polycyclic inhibitors of α-synuclein amyloid assembly. *J. Biol. Chem. 286*, 32036−32044.
(19) Schleucher, J., Schwendinger, M., Sattler, M., Schmidt, P., Schedletzky, O., Glaser, S. J., Sørensen, O. W., and Griesinger, C. (1994) A general enhancement scheme in heteronuclear multidimensional NMR employing pulsed field gradients. *J. Biomol. NMR 4*, 301−306.
(20) Pervushin, K. V., Wider, G., and Wüthrich, K. (1998) Single Transition-to-single Transition Polarization Transfer (ST2-PT) in [^{15}N,^{1}H]-TROSY. *J. Biomol. NMR 12*, 345−348.
(21) Delaglio, F., Grzesiek, S., Vuister, G. W., Zhu, G., Pfeifer, J., and Bax, A. (1995) NMRPipe: a multidimensional spectral processing system based on UNIX pipes. *J. Biomol. NMR 6*, 277−293.
(22) Vranken, W. F., Boucher, W., Stevens, T. J., Fogh, R. H., Pajon, A., Llinas, M., Ulrich, E. L., Markley, J. L., Ionides, J., and Laue, E. D. (2005) The CCPN data model for NMR spectroscopy: development of a software pipeline. *Proteins 59*, 687−696.
(23) Findeisen, M., Brand, T., and Berger, S. (2007) A ^{1}H-NMR thermometer suitable for cryoprobes. *Magn. Reson. Chem. 45*, 175−178.
(24) Danielsson, J., Jarvet, J., Damberg, P., and Gräslund, A. (2002) Translational diffusion measured by PFG-NMR on full length and fragments of the Alzheimer Aβ(1−40) peptide. Determination of hydrodynamic radii of random coil peptides of varying length. *Magn. Reson. Chem. 40*, S89−S97.
(25) Johnson, C. S. J. (1999) Diffusion ordered nuclear magnetic resonance spectroscopy: principles and applications. *Prog. Nucl. Magn. Reson. Spectrosc. 34*, 203−256.
(26) Huang, H., Milojevic, J., and Melacini, G. (2008) Analysis and optimization of saturation transfer difference NMR experiments designed to map early self-association events in amyloidogenic peptides. *J. Phys. Chem. B 112*, 5795−5802.
(27) Mayer, M., and Meyer, B. (1999) Characterization of ligand binding by saturation transfer difference NMR spectroscopy. *Angew. Chem., Int. Ed. 38*, 1784−1788.
(28) Hwang, T.-L., Mori, S., Shaka, A. J., and van Zijl, P. C. M. (1997) Application of phase-modulated CLEAN chemical EXchange Spectroscopy (CLEANEX-PM) to detect water-protein proton exchange and intermolecular NOEs. *J. Am. Chem. Soc. 119*, 6203−6204.
(29) Hwang, T.-L., van Zijl, P. C. M., and Mori, S. (1998) Accurate quantitation of water−amide proton exchange rates using the Phase-Modulated CLEAN chemical EXchange (CLEANEX-PM) approach with a Fast-HSQC (FHSQC) detection scheme. *J. Biomol. NMR 11*, 221−226.
(30) Danielsson, J., Jarvet, J., Damberg, P., and Gräslund, A. (2005) The Alzheimer β-peptide shows temperature-dependent transitions between left-handed 3-helix, β-strand and random coil secondary structures. *FEBS J. 272*, 3938−3949.
(31) Litman, B. J. (1972) Effect of light scattering on the circular dichroism of biological membranes. *Biochemistry 11*, 3243−3247.
(32) Buell, A. K., Dobson, C. M., Knowles, T. P., and Welland, M. E. (2010) Interactions between amyloidophilic dyes and their relevance to studies of amyloid inhibitors. *Biophys. J. 99*, 3492−3497.
(33) Kirkitadze, M. D., Condron, M. M., and Teplow, D. B. (2001) Identification and characterization of key kinetic intermediates in amyloid β-protein fibrillogenesis. *J. Mol. Biol. 312*, 1103−1119.
(34) Jarvet, J., Danielsson, J., Damberg, P., Oleszczuk, M., and Gräslund, A. (2007) Positioning of the Alzheimer Aβ(1−40) peptide in SDS micelles using NMR and paramagnetic probes. *J. Biomol. NMR 39*, 63−72.
(35) Bokvist, M., Lindström, F., Watts, A., and Gröbner, G. (2004) Two types of Alzheimer's β-amyloid (1−40) peptide membrane interactions: aggregation preventing transmembrane anchoring versus accelerated surface fibril formation. *J. Mol. Biol. 335*, 1039−1049.
(36) Rangachari, V., Moore, B. D., Reed, D. K., Sonoda, L. K., Bridges, A. W., Conboy, E., Hartigan, D., and Rosenberry, T. L. (2007) Amyloid-β(1−42) rapidly forms protofibrils and oligomers by distinct pathways in low concentrations of sodium dodecylsulfate. *Biochemistry 46*, 12451−12462.
(37) Tew, D. J., Bottomley, S. P., Smith, D. P., Ciccotosto, G. D., Babon, J., Hinds, M. G., Masters, C. L., Cappai, R., and Barnham, K. J. (2008) Stabilization of neurotoxic soluble β-sheet-rich conformations of the Alzheimer's disease amyloid-β peptide. *Biophys. J. 94*, 2752−2766.
(38) Barghorn, S., Nimmrich, V., Striebinger, A., Krantz, C., Keller, P., Janson, B., Bahr, M., Schmidt, M., Bitner, R. S., Harlan, J., Barlow, E., Ebert, U., and Hillen, H. (2005) Globular amyloid β-peptide oligomer - a homogenous and stable neuropathological protein in Alzheimer's disease. *J. Neurochem. 95*, 834−847.
(39) Fezoui, Y., and Teplow, D. B. (2002) Kinetic studies of amyloid β-protein fibril assembly. Differential effects of α-helix stabilization. *J. Biol. Chem. 277*, 36948−36954.
(40) Nerelius, C., Sandegren, A., Sargsyan, H., Raunak, R., Leijonmarck, H., Chatterjee, U., Fisahn, A., Imarisio, S., Lomas, D. A., Crowther, D. C., Strömberg, R., and Johansson, J. (2009) α-helix targeting reduces amyloid-β peptide toxicity. *Proc. Natl. Acad. Sci. U. S. A. 106*, 9191−9196.
(41) Sandberg, A., Luheshi, L. M., Söllvander, S., Pereira de Barros, T., Macao, B., Knowles, T. P., Biverstål, H., Lendel, C., Ekholm-Petterson, F., Dubnovitsky, A., Lannfelt, L., Dobson, C. M., and Härd, T. (2010) Stabilization of neurotoxic Alzheimer amyloid-β oligomers by protein engineering. *Proc. Natl. Acad. Sci. U. S. A. 107*, 15595−15600.
(42) Chiti, F., Stefani, M., Taddei, N., Ramponi, G., and Dobson, C. M. (2003) Rationalization of the effects of mutations on peptide and protein aggregation rates. *Nature 424*, 805−808.
(43) Ryan, T. M., Griffin, M. D., Teoh, C. L., Ooi, J., and Howlett, G. J. (2011) High-affinity amphipathic modulators of amyloid fibril nucleation and elongation. *J. Mol. Biol. 406*, 416−429.
(44) Kim, W., and Hecht, M. H. (2006) Generic hydrophobic residues are sufficient to promote aggregation of the Alzheimer's Aβ42 peptide. *Proc. Natl. Acad. Sci. U. S. A. 103*, 15824−15829.
(45) Pawar, A. P., Dubay, K. F., Zurdo, J., Chiti, F., Vendruscolo, M., and Dobson, C. M. (2005) Prediction of "aggregation-prone" and "aggregation-susceptible" regions in proteins associated with neurodegenerative diseases. *J. Mol. Biol. 350*, 379−392.
(46) Frid, P., Anisimov, S. V., and Popovic, N. (2007) Congo red and protein aggregation in neurodegenerative diseases. *Brain Res. Rev. 53*, 135−160.
(47) Kim, Y. S., Randolph, T. W., Manning, M. C., Stevens, F. J., and Carpenter, J. F. (2003) Congo red populates partially unfolded states of an amyloidogenic protein to enhance aggregation and amyloid fibril formation. *J. Biol. Chem. 278*, 10842−10850.
(48) Rudyk, H., Vasiljevic, S., Hennion, R. M., Birkett, C. R., Hope, J., and Gilbert, I. H. (2000) Screening Congo red and its analogues for their ability to prevent the formation of PrP-res in scrapie-infected cells. *J. Gen. Virol. 81*, 1155−1164.
(49) Sabaté, R., and Estelrich, J. (2005) Stimulatory and inhibitory effects of alkyl bromide surfactants on β-amyloid fibrillogenesis. *Langmuir 21*, 6944−6949.
(50) Knowles, T. P., Waudby, C. A., Devlin, G. L., Cohen, S. I., Aguzzi, A., Vendruscolo, M., Terentjev, E. M., Welland, M. E., and

Dobson, C. M. (2009) An analytical solution to the kinetics of breakable filament assembly. *Science 326*, 1533−1537.
(51) Cohen, S. I., Vendruscolo, M., Welland, M. E., Dobson, C. M., Terentjev, E. M., and Knowles, T. P. (2011) Nucleated polymerization with secondary pathways. I. Time evolution of the principal moments. *J. Chem. Phys. 135*, 065105.
(52) Cohen, S. I., Vendruscolo, M., Dobson, C. M., and Knowles, T. P. (2011) Nucleated polymerization with secondary pathways. II. Determination of self-consistent solutions to growth processes described by non-linear master equations. *J. Chem. Phys. 135*, 065106.
(53) Cohen, S. I., Vendruscolo, M., Dobson, C. M., and Knowles, T. P. (2011) Nucleated polymerization with secondary pathways. III. Equilibrium behavior and oligomer populations. *J. Chem. Phys. 135*, 065107.